International Journal of Greenhouse Gas Control 96 (2020) 103010

Contents lists available at ScienceDirect

International Journal of Greenhouse Gas Control

journal homepage: www.elsevier.com/locate/ijggc

Review of modelling and simulation strategies for evaluating corrosive behavior of aqueous amine systems for CO_2 capture

Shaukat Ali Mazari[a,*], Lubna Ghalib[b], Abdul Sattar[a], Mir Muhammad Bozdar[a], Abdul Qayoom[a], Israr Ahmed[c], Atta Muhammad[a], Rashid Abro[a], Ahmed Abdulkareem[d], Sabzoi Nizamuddin[e], Humair Baloch[e], N.M. Mubarak[f]

[a] Department of Chemical Engineering, Dawood University of Engineering and Technology, Karachi 74800, Pakistan
[b] Materials Engineering Department, Mustansiriayah University, 14022 Baghdad, Iraq
[c] School of Chemical Engineering, University of Faisalabad, Faisalabad, Pakistan
[d] Mathematics Science, Directorate General of Education Rusafa 1, Baghdad, Iraq
[e] School of Engineering, RMIT University, Melbourne 3000, Australia
[f] Department of Chemical Engineering, Faculty of Engineering and Science, Curtin University, 98009 Sarawak, Malaysia

ARTICLE INFO

Keywords:
Corrosion models
Carbon steel corrosion
Electrochemical reactions
CO_2 corrosion
CO_2 capture
Polarization curve

ABSTRACT

Corrosion is one of the critical problems for process operations and plant life. Amine-based post-combustion CO_2 capture systems are known to be corrosive. This is because of the absorption of CO_2 by aqueous amine solution, which makes the system acidic and generates oxidizing agents through ionization leading to corrosion. Corrosion increases with CO_2 loading, process temperature, presence of oxygen (O_2), occurrence of sulfur compounds, low pH, velocity of solution and formation of some degradation products. Conducting experimental investigations to determine the rate of corrosion at various parts of process plant under a wide range of operating parameters is difficult and costly. Mathematical models and simulations play an important role in estimating the rate of corrosion under wide range of operating parameters for such systems. This study highlights the process of corrosion for amine-based CO_2 capture systems and development of corrosion models with critical analyses on their applications. Study also highlights the outlook of models and simulations.

1. Introduction

Industrialization, specially the coal dependency for energy is not going anywhere soon. Matter of the fact is that at present there is a list of 10,000 retired, operating and planned coal units, producing a total of almost 3,000 GW in 95 countries (Evans and Rosamund, 2019). It is reported that China and India are the leading countries with installation of new coalfired power plants in last decade. Installation of new coal-fired power plants are reported to further thicken the atmospheric carbon dioxide (CO_2) layer beyond the repair. Records of Mauna LOA Observatory indicate that very unfortunately we already have crossed the mark of 415 ppm of CO_2 in atmosphere in May 2019 (Observatory, 2019). CO_2 is one the major greenhouse gases and it tends to accumulate in atmosphere leading to global warming and climate change. This means that the need for a retrofit technology for CO_2 capture cannot be ignored.

History of use of amines for sour gas treatment goes back to 1930s (Roger, 1930, 1931). The technology uses amines to capture CO_2 and sulfur dioxide (SO_2). The technology has already matured on sour natural gases treatment before its application for CO_2 capture from flue gases (Milton, 1963). Retrofitting option of post-combustion CO_2 capture technology makes it feasible for CO_2 capture from flue gases (Rochelle, 2009). However, process operating conditions differ in flue gas treatment than natural gas (Gao et al., 2012; Soosaiprakasam, 2007; Wattanaphan et al., 2013). The amine-based CO_2 absorption is a chemical process. Mass transfer takes place between the gas and the liquid phase. The tall absorber and desorber vessels are used for the absorption and desorption. The major equipment involved in amine-based absorption process are absorber also called scrubber, regenerator also called stripper and desorber, rich-lean solution cross heat exchanger, reboiler, overhead condenser and cooler. A typical amine-based absorption process is exhibited in Fig. 1.

The emitted flue gases from coalfired power plants are cooled before their entry to the major process equipment to enhance absorption efficiency and lower the risk of escape and degradation of solvent. In the process, aqueous amine reacts with CO_2 to produce water soluble ions,

* Corresponding author.
E-mail address: shaukat.mazari@duet.edu.pk (S.A. Mazari).

https://doi.org/10.1016/j.ijggc.2020.103010
Received 22 September 2019; Received in revised form 31 January 2020; Accepted 28 February 2020

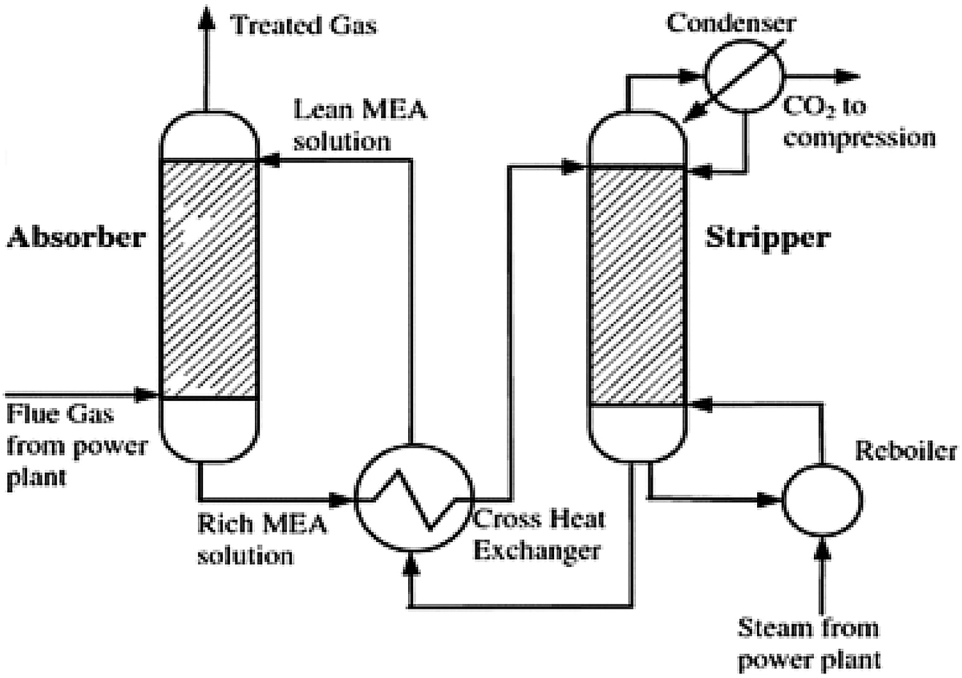

Fig. 1. Process flow diagram of amine-based CO_2 capture technology (Oko et al., 2017).

even at low CO_2 partial pressure. Equilibrium plays a vital role in defining CO_2 capture operating capacity of the amine (Mandal et al., 2001). Amines are known for their faster CO_2 absorption kinetics (Chakma, 1997). The hydroxyl group in an amine reduces the vapor pressure and increases water solubility, whereas amino group facilitates alkalinity in aqueous solution (Kohl and Nielsen, 1997). Monoethanolamine (MEA), diethanolamine (DEA), diglycolamine (DGA), diisopropanolamine (DIPA), triethanolamine (TEA), piperazine (PZ), 2-amino-2-methyl-1-propanol (AMP), methyldiethanolamine (MDEA) are commonly tested and tried amines for CO_2 absorption. However, MEA, DEA, DGA, PZ and MDEA have gained the commercial or large interest (Kohl and Nielsen, 1997; Mazari et al., 2014, 2015; Saeed et al., 2018). Among others, MEA is the most widely tested and tried amine for CO_2 capture application (DuPart et al., 1993; Luis, 2016; Saeed et al., 2018).

One of the major issues associated with amine-based CO_2 capture technology is the corrosion. Corrosion not only reduces equipment life but also troubles the process. Corrosion involves electrochemical reactions under acidic conditions. Hot parts of the CO_2 capture plant undergo higher corrosion rates compared to cold ones under the influence of CO_2 (Kittel et al., 2009). This indicates a direct relation of CO_2 concentration and temperature with the rate of corrosion. Furthermore, other parameters like accumulation of heat stable salts or degradation products like bicine, presence of oxygen, solution velocity and type of amine also influence the rate of corrosion (Liang et al., 2016). Measuring corrosion for each equipment at multiple locations with changing process conditions is a difficult and costly task. Modelling and simulation methods can help in estimating the rate of corrosion at different parts of equipment under varied process operating conditions. Several authors have developed corrosion rate models for CO_2 environments using experimental data and mathematical frameworks, even computational studies using molecular modelling (Kahyarian et al., 2017; Liu and Zheng, 2008). Empirical, semi-empirical, elementary mechanistic models and comprehensive mechanistic models are commonly used for the prediction of rate of corrosion in aqueous-amine-CO_2 systems. Every model has limitations; however, several models have good predictability. There are no such studies in open domain literature, which explain the modelling strategies for corrosion rate of process equipment in carbonated aqueous amine systems. Hence, this study aims to bridge the gap by highlighting corrosion rate model development strategies, their applicability and limitations.

2. Corrosion in amine-based CO_2 capture plants

Corrosion causes operating problems, reduces equipment and plant life, and impeaches safety protocols, which are directly related to overall economics of the plant (Kohl and Nielsen, 1997). Corrosion can also cause unscheduled downtime of plant, reduced equipment life, losses in production, and invoke the possibility of human health (Murata et al., 2015). Amine-based gas treating plants are constructed of carbon steel, which are susceptible to corrosion induced by CO_2 activated ions of water and amine (DuPart et al., 1993). Corrosion rate varies with plant location due to different local operating conditions. However, the severe corrosion is observed in absorber bottom, regenerator areas (trays and valves), rich-lean solution heat exchanger, reboiler (in some cases) and associated piping (DuPart et al., 1993). There are two major types of corrosion for amine-based CO_2 capture process, wet CO_2 corrosion and amine solution corrosion.

2.1. Wet CO_2 corrosion

Presence of CO_2 in the process causes wet acid gas or CO_2 corrosion, which can prevail even with little or without amine solution (Kohl and Nielsen, 1997). Amine solvents are alkaline in nature, which hinders the process of corrosion. However, at lower concentrations or in the absence amine, CO_2 makes water solution highly acidic, which leads to severe corrosion. Due to water saturation in feed gas bottom of the absorber and overhead sections of the regenerator are more susceptible to situations where wet CO_2 corrosion can take place (Kohl and Nielsen, 1997). Amine spray may be introduced to the overhead of the regenerator to reduce the corrosion. Similarly, bottom of the absorber may be wetted with amine to elevate the pH of the susceptible locations to reduce the CO_2 corrosion (Dugstad, 1998; Dugstad et al., 2003; Kohl and Nielsen, 1997). Wetting of the absorber bottom may be achieved by immersing the inlet gas distributor in the amine solution. Similarly, drilling weep holes by the perimeter of the bottom tray support ring can be another option with better operability. Another option may be changing the material of construction of absorber bottom, where stainless steel has shown good corrosion resistance (Najumudeen,

2012).

2.2. Amine solution corrosion

Amines and their aqueous solutions are not corrosive in nature due to higher alkalinity. However, amines react with CO_2 to form carbamate species, including oxidizing agents and creating an acidic environment, which lead to corrosion (Kohl and Nielsen, 1997). Amine solution corrosion takes place mostly in piping sections of the rich solution, the rich amine side of the lean-rich solution heat exchanger, at the bottom of the absorber to the regenerator, and at the hot bottom part of the regenerator. Severity of the corrosion depends on the type and concentration of amine solution, oxygen ingression, temperature, CO_2 loading, amine degradation products and the solution contamination. Moreover, plant design and its material of construction, equipment fabrication, routine operating practices and procedures also influence the amine solution corrosion (Kohl and Nielsen, 1997).

CO_2 loading increases the rate of corrosion as direct reduction of bicarbonates increases due to of HCO_3^- and H^+ ion concentration in the solution. (De Waard and Milliams, 1975) reported that the rate corrosion of carbon steel increases as partial pressure of CO_2 (P_{CO2}) increases. Similar relations of rate of corrosion and P_{CO2} are reported in different studies (Feng et al., 2012). Increase in temperature also increases the rate of corrosion (DuPart et al., 1991; Helle, 1995; Keller et al., 1992; Veawab et al., 1999). CO_2 loading is reported to form protective layer of intermediate Chukanovite leading to siderite (Zheng et al., 2016a). This means initially with increase in CO_2 loading, the rate of corrosion increases but once protective layer is formed it inhibits the corrosion. Reactions are temperature dependent as per Arrhenius relation of temperature and chemical kinetics. Hence, increase in temperature shall increase the rate of chemical and electrochemical reactions participating in mass transport and rate of corrosion. This is worth noticing that the amine-based absorption-desorption process temperatures vary from 40 to 120 °C depending upon the application of amine. At elevated temperatures, amines along with their degradation products like Bicine, Formic Acid, Oxalic Acid, Acetic Acid, N-(2-hydroxyethyl) ethylenediamine, N-(2-hydroxyethyl)- glycine, N-(2-hydroxyethyl)- acetamide etc. act as corrosion agents (Fytianos et al., 2016).

Apart from CO_2 loading and process temperature, amine concentration is also considered an important aspect of corrosion studies. Generally, it has been observed and reported that the corrosion rate of material of construction increases with increase in amine concentration (Chakma and Meisen, 1986; DuPart et al., 1991; Veawab et al., 1999). (Tanthapanichakoon and Veawab, 2003) reported that higher concentration of amine is preferred in industry over lower concentration due to energy saving. Recommendations on the selection of amine concentration to limit the rate of corrosion are also available in literature (Nielsen et al., 1995).

Velocity of solution influences the transfer of oxidizing agents between the carbonated solution and the metal surface, which results an increase in rate of corrosion of the metal. This suggests that when film formation does not take place, the rate of corrosion of metal totally depends on the solution velocity (Videm and Dugstad, 1989). Similarly, the film gets detached or vanishes due to solution velocity, which can upsurge the corrosion rate of material of construction (Nešić, 2007). Film layer plays a dual job, it not only resists the mass transfer of oxidizing species, but also resists the rate of corrosion by itself.

3. Mechanism of solution corrosion

3.1. CO_2 corrosion pathway

Formation of bicarbonate ion (HCO_3^-) and hydrogen ion (H^+) (R2) takes place through the ionization of carbonic acid (H_2CO_3) when CO_2 is dissolved in water (R1) (Nešić et al., 2002; Nyborg, 2002).

$$CO_2 + H_2O \rightleftharpoons H_2CO_3 \quad (1)$$

$$H_2CO_3 \rightleftharpoons H^+ + HCO_3^- \quad (2)$$

Increase in H^+ ions concentration increases wet corrosion of material of construction. H^+ accepts electrons from iron (Fe), which leads to oxidation of Fe to Fe ions (Fe^{+2}) and thereby producing hydrogen gas (H_2) as per reaction (3).

$$2H^+ + Fe \rightarrow Fe^{+2} + H_2 \quad (3)$$

Reduction of bicarbonate ions takes place by the formation of carbonate ions (CO_3^{-2}) at pH values higher than 4. This leads to the formation of more hydrogen ions, which enhances the rate of corrosion reaction (4) (Nesic et al., 2001b).

$$HCO_3^- \rightleftharpoons CO_3^{-2} + H^+ \quad (4)$$

Chemical reactions are temperature sensitive. Reaction (4) involves the concentration of CO_2, this suggests that temperature and CO_2 loading shall increase the rate of reaction and hence rate of corrosion (Kohl and Nielsen, 1997).

3.2. Amine-CO_2 corrosion pathway

The amine-CO_2 corrosion has a different pathway than CO_2 corrosion, however it is not understood completely yet. Riesenfeld and Blohm (1950) reported that acid gases from rich amine solutions cause the corrosion, where in the presence of water, CO_2 reacts with an iron surface to produce iron carbonate ($FeCO_3$) as per reaction (5)

$$Fe + CO_2 + H_2O \rightarrow FeCO_3 + H_2 \quad (5)$$

It has been established that amine-CO_2 causes the exit of the proton from the amine solution for carbon steel corrosion as shown in reactions (6) and (7) (Kosseim, 1984).

$$CO_2 + R_3N + H_2O \rightleftharpoons R_3NH^+ + HCO_3^- \quad (6)$$

$$CO_2 + 2R_2NH \rightleftharpoons R_2NH_2^+ + R_2NCO_2^- \quad (7)$$

Hydrogenated amine ions ($R_2NH_2^+$ and R_3NH^+) provide protons for the corrosion reaction and are acidic in nature. The corrosion infected carbon steel has tendency to react with the acid present in the solution. Amine solutions indicate a higher number of the protonated ions compared to hydrogen ions. The reaction mechanism may be illustrated as under (reactions 8 and 9):

$$Fe + 2R_3NH^+ \rightleftharpoons Fe^{+2} + H_2 + 2R_3N \quad (8)$$

$$Fe + 2R_2NH_2^+ \rightleftharpoons Fe^{+2} + H_2 + 2R_2NH \quad (9)$$

Corrosion rate increases with increase in concentration of protonated amine. Moreover, it is also established that solutions with higher CO_2 concentration have higher corrosion potential than that of a lean solution (Kohl and Nielsen, 1997). Carbamate species are suspected corrosion agents. Tertiary amines do not produce carbamate ions and are less corrosive compared to primary and secondary amines (DuPart et al., 1993). To determine the oxidizing agents, (Veawab and Aroonwilas, 2002) developed a mechanistic model for aqueous MEA based CO_2 system. Authors found HCO_3^- and H_2O as the major oxidizing agents. Likewise, the same oxidizing agents are reported for aqueous DEA based CO_2 system (Benamor and Al-Marri, 2014). For aqueous MDEA based CO_2 system, $MDEAH^+$ and HCO_3^- ions are suggested as strong oxidizing agents compared to H_2O and H_3O^+ ions (Choi et al., 2012). These results are also supported by the investigation of (Duan et al., 2013).

4. History of corrosion models for amine-based CO_2 systems

4.1. Models for CO_2 corrosion

Researchers started developing models for predicting the rate of

corrosion for CO_2 capture systems since 1970s. The model of De Waard and Milliams (1975) is one of the very commonly accepted models for estimating the rate of corrosion for CO_2 absorption systems. Several corrosion rate models then followed with time through the same research group (De Waard and Lotz, 1993; De Waard et al., 1995, 1991; De Waard and Milliams, 1975; Pots et al., 2002). Majority of the initial corrosion rate models were based on CO_2 environments in oil and gas industry. Direct reduction of H_2CO_3 is assumed in these developed mechanistic models and correlated with data obtained from glass cell reactors at laboratory scale. As shown in Eq. (10), the corrosion rate depends only on temperature and effect of CO_2 partial pressure (10):

$$\log(\mathrm{CR}) = 7.96 - \frac{2320}{\mathrm{T}+273} - 0.00555\ \mathrm{T} + 0.67\log\left(\mathrm{P}_{\mathrm{CO_2}}\right) \tag{10}$$

Where T is the temperature (°C), CR is the rate of corrosion in millimeters per year (mmpy) and P_{CO2} is the CO_2 partial pressure (bars). The Arrhenius type equation has been used to analyze the effect of temperature, which provided the temperature function as shown in Eq. (10). H^+ ions form in solution due to detachment of carbonic acid assuming pure saturated CO_2 solution. Based on this assumption, CO_2 partial pressure function is added in Eq. (10). The influence of concentration of OH^- ions is misleadingly as it indicates that it will strongly effect the anodic dissolution of iron. Whereas, on the other hand it is a pH dependent mechanism (Bockris et al., 1961) and is only valid in strong acidic solutions (pH < 4) (Lee, 2004).

Later on, De Waard et al. (1991) improved their model by adding effect of other parameters on the rate of corrosion like flow velocity, pH, protective iron carbonate ($FeCO_3$) film formation, mass transport and steel composition. Eq. (11) represents the revised model for predicting the rate of corrosion and fitted on the nomogram. The developed nomogram for the same model helped in determining the amended corrosion rate.

$$\log(\mathrm{CR}) = 5.8 - \frac{1710}{\mathrm{T}} + 0.67\log(\mathrm{P}_{CO_2}) \tag{11}$$

Another empirical corrosion model based on chemical reaction kinetics principles was developed by Mishra et al. (1997). The model considers temperature, CO_2 partial pressure and pH (concentration of H^+) as shown in Eq. (12).

$$CR = C\,H^{+1.33}\,P_{CO_2}^{0.67}\,e^{-Q/kT} \tag{12}$$

Where C is a constant, CR is the rate of corrosion rate (mm/yr), P_{CO2} denotes the partial pressure of CO_2 in (N/m^2), [H^+] is the concentration of H^+ ions ($kmol/m^3$), k is the Boltzmann constant (J/K), and Q is the instantaneous rate of reaction constant for CO_2 dissolution in water.

A corrosion rate model based on thermodynamic and electrochemical mechanisms was developed by Anderko and Young (1999). The model provides an anodic and cathodic processes at the metal surface and a realistic speciation of aqueous system. Experimental data has been used to validate the predicted results on the rate of corrosion against parameters like temperature, solution composition, CO_2 partial pressure and flow velocity. Nesic et al. (2001a) developed another mechanistic corrosion rate model for aqueous CO_2 system. Several operating parameters like diffusion of chemical species between bulk and metal surface, electrochemical reactions at the metal surface, electromigration of ions under the influence of the established potential gradients, diffusion of chemical species across porous $FeCO_3$ corrosion films, and the chemical reactions happening in the bulk solution have been incorporated in the model. To study the effect of $FeCO_3$ film thickness the user may define the values to investigate the effect on the rate of corrosion. The model later was improvised by Nešic and Lee (2003) by adding growth of $FeCO_3$ films into the model. The supersaturation of Fe^{2+} and CO_3^{2-} ions causes $FeCO_3$ precipitation. It has been established from the models that high pH values, high CO_2 partial pressure, high temperature, and high Fe^{2+} concentration contributes to the formation of $FeCO_3$ films. The mechanistic models also incorporate species transport to determine speciation concentration (Nešić et al., 2009). To predict the rate of corrosion of carbonated systems, such models addon the effects of H_2S, O_2 and organic acids. Speciation concentration was determined by using Fick's first and second laws and electro-neutrality. Using this model corrosion rate can be predicted at various temperatures, CO_2 partial pressures, $FeCO_3$ film thicknesses, and flow velocities.

4.2. Models for amine solution corrosion

Veawab and Aroonwilas (2002) developed a model for amine solution corrosion for MEA-H_2O-CO_2 environments. The model incorporates electrochemical reactions on the metal-solution interface and thermodynamic equilibrium of chemical species in bulk solution. The electrolyte Non-Random Two Liquid (NRTL) model was used for the approximation of equilibrium concentration of the chemical species in the solution. To signify kinetics of electrochemical reactions on the metal-solution interface through corrosion processes, the mixed potential theory was used. H_3O^+ ions were found to play only a minor role in corrosion rate, however HCO_3^- and H_2O were identified as the major oxidizing agents. A semi-empirical corrosion prediction model for DEA-H_2O-CO_2 system was developed by Nouri et al. (2008), which is a modification of the earlier corrosion rate model of De Waard and Milliams (1975). Authors used the corrosion rate determined by De Waard and Milliams (1975) model as the base corrosion rate (CR_{base}). However, the improvised corrosion rate (CR_{imp}) was the product of individual correction factors for the effects of all key variables like partial pressure of CO_2 and H_2S, temperature, H_2S/CO_2 ratio, presence of protective films, pH, free water, oil wetting, water composition, presence of methanol and glycol, material type, addition of corrosion inhibitors and the base corrosion rate (CR_{base}). Eq. (13) has been used to estimate the base corrosion rate and improvised corrosion rate is estimated by using Eq. (14).

$$\log CR = 5.8 - \frac{1710}{T} + 0.67\log P_{CO_2} \tag{13}$$

$$\mathrm{CR}_{imp} = \mathrm{CR}_{\mathrm{base}} \prod_{\mathrm{i}=1}^{\mathrm{n}} f_{\mathrm{i}} \tag{14}$$

Where f_i is the correction factor of the i^{th} key effecting variable and n is the total number of key variables. In this research the experimental data were obtained from plant or laboratory for correction factors of all the key influencing parameters.

(Najumudeen, 2012) improvised the mechanistic corrosion rate model for carbon steel of (Veawab and Aroonwilas, 2002) for MEA-CO_2 capture system. Dissolved O_2, $FeCO_3$ film on the metal surface and heat stable salts were included in the model. To calculate the thermodynamic equilibrium concentration of chemical species, present in the solution, researchers used the VLE and e-NRTL sub-model. It was reported that oxidizing agents like H_2O and HCO_3^- contribute more to the rate of corrosion compared to H_3O^+ ions in an aqueous MEA-CO_2 environment. MEA concentration is found to contribute less in the magnitudes of corrosion rate compared to temperature changes and CO_2 loading. Presence of acetic acid (tested as the Heat Stable Salts) and dissolved O_2 in aqueous MEA-CO_2 environments are reported not to affect the rate of corrosion of carbon steel. However, heat stable salts like oxalate, malonate and formate are reported to contribute to the rate of corrosion in a descending order (Tanthapanichakoon et al., 2006). (Choi et al., 2012) developed another corrosion rate estimation model for carbon steel in an aqueous MDEA-CO_2 system. The model was based on key electrochemical reactions and estimation of solution speciation. It has been reported that corrosion rate increases with the rise in HCO_3^- and $MDAH^+$ concentrations. In the absence of protective films, the model can be applied to uniform corrosion.

5. Modelling and simulation strategies for corrosion estimation

5.1. Electrochemical behavior of corrosion

In a medium where conducting ions are present, electrochemical nature of corrosion shall control the rate of corrosion of metals and alloys. Electrochemical corrosion process shall involve the transfer of electrons at the metal-solution interface. Dominant cathodic and anodic reactions shall take part in the mechanism. An anodic reaction is also called the oxidation of any chemical specie, which gives away an electron (e^-) to become a positively charged ion. On the other hand, cathodic reactions are opposite to anodic reactions. In these reactions, reduction of chemical species takes place by accepting an electron (e^-) to become negatively charged (Yang, 2008).

5.1.1. Electrode potentials

Thermodynamics is involved when energy changes occur during the electrochemical reactions. Electrode potentials play an important role in estimating the rate of reactions and their spontaneity. Laws of thermodynamics can be used in determining the possibility of corrosion reactions; however, they cannot predict the rate of corrosion reactions. Kinetics of electrochemical reactions can be used to estimate the rate of corrosion (Yang, 2008). The cathodic and anodic reactions will start in an electrolysis cell, when any conducting metal is immersed in an ionic electrolyte present in the cell. Electromotive force (emf) or half-cell electrode potential of reaction disburses for each reaction, which is distinct and inherent for each reaction. The variance in the potential of the two half-cell reactions is called electrochemical potential or the cell potential (E) as shown in expression (15):

$$E = E_a + E_c \tag{15}$$

Where, Ec and Ea are cathodic and anodic half-cell electrode potentials respectively.

Change of free energy is associated for any electrochemical reaction. To express the relation between the change in free energy, also known as Gibbs free energy (ΔG), due to electrochemical potential, Eq. (16) may be used.

$$\Delta G = -nFE \tag{16}$$

Where F is the Faraday's constant, (96,485 coulombs per mole), n is the number of electrons traded during reaction, E is the electrochemical potential (V) and ΔG is the Gibb's free energy change (kJ/mol) (Bard and Faulkner, 1980).

5.1.2. Nernst equation

Let us take an example reaction (17), where A, B, C and D be the reactants and products at the same time with a, b, c, and d as their stoichiometric reaction coefficients respectively in a reversible reaction.

$$aA + bB \leftrightharpoons cC + dD \tag{17}$$

Eq. (18) represents the respective changes in Gibbs free energy at the standard reaction conditions.

$$\Delta G^o = (c\,G_C^o + d\,G_D^o) - (a\,G_A^o + b\,G_B^o) \tag{18}$$

Where, Gibbs free energy at standard conditions (25 °C) in the reaction is denoted by superscript o. Moreover, Eq. (19) presents the changes in Gibbs free energy at nonstandard conditions

$$\Delta G = (c\,G_C + d\,G_D) - (a\,G_A + b\,G_B) \tag{19}$$

Whereas Eq. (20) can be used to determine change in free energy from standard to non-standard conditions.

$$\Delta G - \Delta G^o = c(G_c - G_c^o) + d(G_d - G_d^o) - a(G_a - G_a^o) - b(G_b - G_b^o) \tag{20}$$

To estimate the change in Gibbs free energy the terms on the right-hand side of Eq. (20) can be articulated in terms of activity with respect to the standard state conditions. Let us take an example chemical specie, using its concentration [A], a relationship in change in free energy can be developed as under (21):

$$a(G_A - G_A^o) = RT\ln A^a \tag{21}$$

In Eq. (21), R is the universal gas constant (J/mol.K) and T is the absolute temperature (K). Similarly, by doing the same for all chemical species, Eq. (22) can be developed:

$$\Delta G - \Delta G^0 = RT\ln\frac{[C]^c D^d}{[A]^a [B]^b} \tag{22}$$

Applying the relationship between changes in Gibbs free energy and electrode potential (i.e. $\Delta G^o = -nFE^o$ and $\Delta G = -nFE$ yields:

$$E = E^0 - \frac{RT}{nF}\ln\frac{C^c D^d}{A^a B^b} \tag{23}$$

Where, E^o is the standard electrode potential (V). Expression (23) presents a general form of Nernst's equation. This equation is helpful in determining the electrode potential at nonstandard conditions of an electrochemical reaction.

5.1.3. Electrochemical kinetics

In electrochemical reactions, transfer of electrons take place, which means, rate of reaction in electrochemical reactions depends on the rate of flow of electrons. The rate of flow of electron is called current (I), measured in Amperes. Faraday's laws of electrolysis provide the proportionality between the mass of the substance that reacts electrochemically *(m)* (Jones, 1992). Mass of a substance transformed at an electrode is directly proportional to the quantity of electricity transferred *(Q)* at that electrode during an electrolysis process is stated by Faraday's first law of electrolysis (24).

$$m \propto Q \tag{24}$$

Eq. (24) can be rewritten in the form of current and time as under (25):

$$m \propto It \tag{25}$$

Faraday's second law identifies a direct relationship between mass (m) altered at an electrode and to the element's equivalent weight (z). Where z is the ratio of atomic weight (a) to its valency (n). Following expression (26) may be developed to relate the two quantities:

$$m \propto Z \tag{26}$$

On replacing $\left(Z = \frac{a}{n}\right)$ with m, in Eq. (26) and merging Eqs. (25) and (26) can provide Eq. (27).

$$m = \frac{Ita}{nF} \tag{27}$$

where *F* is the proportionality constant, also called Faraday's constant which is equal to 96485 C/mol. On dividing 27 with time t and area A gives the expression 28 for rate of corrosion Jones, 1992:

$$CR = \frac{m}{tA} = \frac{ai}{nF} \tag{28}$$

Where *i* shows the current density (A/cm^2) $\left(i = \frac{I}{A}\right)$. The rate of corrosion may be determined as a function of current density, which is from 10^{-9} up to several A/cm^2. The following Eq. (29) may be used to determine the rate of corrosion.

$$CR = 0.00327\frac{ai}{nD} \tag{29}$$

Where *CR* is the rate of corrosion rate (mm/yr), D is the density of the metal/material (g/cm^3).

5.1.4. Exchange current density

Characteristics of a reversible electrode reaction are known through the exchange current density. This condition is referred to the current

density at the equilibrium condition. In such a situation, rate of the forward half-cell reaction turns out to be equal to the rate of the backward half-cell reaction. The exchange reaction rate and the current density as per Faraday's law can be expressed in Eq. (30):

$$r_f = r_b = \frac{i_0 a}{nF} \tag{30}$$

In the equation, r_f and r_b show oxidation and reduction reaction rate at equilibrium, respectively, "a" is the atomic weight in g/mol, i_o is the exchange current density (A/m^2), n is the number of electrons exchanged, and F is Faraday's constant (Bockris and Reddy, 1970): Where i_0 is determined by expression (31).

$$i_0 = Fk_c C_A exp\left(\frac{\alpha FE_{rev}}{RT}\right) \tag{31}$$

Where C_A is the concentration of the reactant (kmol/m^3), k_c is the reaction rate constant, α is the symmetry factor, and E_{rev} is the equilibrium potential (V). It must be noted that an instrument cannot measure the absolute values of i_0 as there is no net transfer of electrons. On the other hand, lack of knowledge of reaction rate constant k_c and the polarization curves hinder the theoretical determination of i_0.

5.1.5. Polarization behavior

Electrochemical polarization is the deviation in electrochemical potential from the equilibrium potential. Electrodes without of an external current show the equilibrium potential, which may be measured in voltage units (volts (V)) and millivolts mV. The potential change (E-E_{rev}) is known as polarization (η). Polarization is measures as cathodic and anodic. Addition of electrons from a negative charge accumulate at the cathode causing the cathodic polarization. Whereas, removal of electrons due to a positive charge buildup at the anode resulting anodic polarization (Bockris and Reddy, 1970).

Two categories of electrochemical polarizations are established: activation polarization and concentration polarization. First take place when lower rate of electron transfer at the metal-solution interface occur compared to the rate of chemical species transport from the bulk solution to the interface. Whereas, later happens when rate of electron transfer at the metal-solution interface is larger compared to the rate of chemical species transport from the bulk solution to the interface. The activation polarization influences corrosion rate of the metal to be contingent on rate of electron transfer at the interface. Whereas, the concentration polarization causes corrosion to be instantaneous. In some cases, when both activation and concentration polarizations coexist at the electrode surface, the corrosion will be known as combined polarization (Soosaiprakasam and Veawab, 2008).

5.2. Thermodynamic models

Vapor Liquid Equilibrium (VLE) data is used for thermodynamic models. Acid gases and amines are weak electrolytes. The system dissociates partially into a complex mixture of highly volatile molecular species such as CO_2, nonvolatile solvent species (amine), and nonvolatile ionic species in an aqueous phase. At constant temperature and pressure in a closed system, the phase equilibrium governs the distribution of molecular species between the liquid and vapor phases. Whereas, chemical reactions occur in the liquid phase between acid gases and amines to produce several ionic species. It becomes a complicated process to represent the behavior of vapor-liquid equilibrium (VLE). Hence, this takes both phase and chemical equilibria to represent a proper VLE behavior.

In an open system, due to unlimited supply of gas, there is a constant partial pressure of carbon dioxide gas species on the surface of the solution. When carbon dioxide is dissolved in aqueous solution containing alkanolamines, aqueous carbon dioxide undergoes a sequence of chemical reactions. Vapour liquid equilibrium has been used to calculate the concentration of all species in the solution and activity coefficients for the chemical species to know the concentration of oxidizing agents responsible for the corrosion. The electrochemical corrosion model describes the electrochemical behavior taking place on metal surface that is exposed to aqueous carbonated solutions of alkanolamines. The reactions were assumed to be under mixed potential. The reversible potential for species in the solution is calculated from the Nernst Eq. (32).

$$E_{rev} = E_T^o \frac{RT}{nF} \ln\left(\frac{a_{oxidation}}{a_{reduction}}\right) \tag{32}$$

Several authors have compared results of thermodynamic models with experimental data, which depict a minor deviation. This indicates that corrosivity effaces the VLE, however due to small error, it may be ignored.

Most models assume the activity coefficients for all species to be unity when modelling a VLE behavior of a weak electrolyte solution. Activity coefficient models or semi-empirical excess Gibbs energy models for aqueous electrolyte systems are widely used. Other several thermodynamic models have also been developed to determine the solubility of CO_2 for amine solutions. Major contributions in simulating amine-CO_2 systems come from the three major type of VLE models.

i Empirical approach, based on regression was introduced by Kent and Eisenberg (1976) and Lee et al. (1976). In these models, CO2 partial pressure and solubility data were fitted through equilibrium constants. The equilibrium was based on pseudo-equilibrium constants and Henry's law. To match experimental VLE data, the pseudo-equilibrium constants for amine protonation and carbamate revision reactions for MEA and DEA systems were regressed. In such cases, models were developed with only two parameters per acid gas to determine the ionic strength dependencies of partial pressures of acid gas. It must be noted that such models bring good results for CO_2 loading values higher than 0.1 mol per mol amine. However, ionic species concentrations cannot be estimated using such models.

ii Second category of thermodynamic models include the use of excess Gibbs energy models to estimate the activity coefficients of chemical species. Deshmukh and Mather (1981) developed a thermodynamically rigorous model based on extended Debye-Huckel (Hartley, 1935) theory and the work of Cross et al. (1990); DuPart et al. (1991) and Beutier and Renon (1978). Most importantly, the model has only one term to account for electrostatic forces by Debye-Huckel law, whereas for short range interactions they have another term with adjustable parameters. More sophisticated models were developed based on rigorous physical-chemical properties by others (Austgen et al., 1989; Austgen Jr, 1989) for evaluating liquid phase chemical equilibria of acid gas-aqueous amine (gas-liquid) systems. Such models require input of Henry's constants for gases, the equilibrium constant for all solution reactions, and binary interaction parameters for all important solution species. Austgen et al. (1991) used the electrolyte-NRTL (e-NRTL) model to correlate available data related to acid gas- aqueous amine equilibria. Model parameters for the acid gas-amine-water system, were obtained through the regression of amine-water and CO_2 partial pressure data. The activity coefficients were determined by using the e-NRTL model, which assumes water to have non-ideal behavior. For model development, the binary interaction parameters between all chemical species (including water) were considered (Austgen et al., 1989; Mock et al., 1986). Similarly, Zheng et al. (2016b) used e-NRTL model to determine the speciation concentration for the development of thermodynamic models for corrosion of AMP and MEA. Study reported formation of protective $FeCO_3$ due to the concentration of HCO_3^- ions. Model results were compared with the experimental data of Ciftja et al. (2011), which showed good agreement.

iii The third category of VLE models is the application of equations of

state (EOS) to represent both liquid and vapor phases of the system. These models are effective in estimating the activity coefficients of chemical species under varying temperatures and pressures for binary and multicomponent VLE systems (Aronu et al., 2011; Mac Dowell et al., 2013).

5.3. Modeling the kinetics of aqueous corrosion

In the aqueous corrosion, electrochemical reactions involve charge transfers at metal-solution interface, which makes a heterogeneous system. This involves: the reactions taking place in the bulk aqueous system, charge transfer at the metal surface to produce products, transport of reactants to the metal surface, release of produced products at the surface, transport of products into bulk of the solution. Investigations on aqueous corrosion kinetics help in determining and understanding quantitative and qualitative influence of external conditions, fluid velocity, solution chemistry and metallurgical physiognomies of the corroding interface on the rate of electrochemical corrosion.

Corrosion potential and rate of corrosion are considerable constraints in developing an electrochemical model. Knowing corrosion rate helps in determining the rate of dissolution in obstructed environments like pits or crevices and in simulating general corrosion patterns. Whereas, corrosion potential plays an important role in determining the type of corrosion damage. Hence, the corrosion model should be able to facilitate instantaneously a rational corrosion potential and corrosion rate. Further, computational investigations on the corrosion potential may also be useful in estimating the rate of corrosion (Anderko, 2010).

5.3.1. Modeling the charge transfer

Vetter (2013); Bockris and Reddy (1970); Kaesche (1985); Bockris and Khan (2013); Gileadi (1993) and several others reviewed the developed theory of charge transfer reactions.

In electrochemical reactions, where charge transfer takes place between two species, shall form reduced (Red) and oxidized (Ox) species simultaneously, as per Eq. (33):

$$\mathrm{Red} \underset{r_c}{\overset{r_a}{\rightleftharpoons}} \mathrm{Ox} + ne \tag{33}$$

The difference between anodic rate (v_a) and cathodic rate (v_c), multiplied by nF as shown in Eq. (33) provides the current density for the reaction (34).

$$i = nF(v_a - v_c) \tag{34}$$

The rates of anodic and cathodic reactions are related to the potential and the concentration of the reacting species at phase boundary, as shown in Eq. (35) (Vetter, 2013).

$$i_a = nFv_a = nFk_a C_{r,s}^{x,r} exp\left(\frac{\alpha_a nFE}{RT}\right) \tag{35}$$

Eq. (35) can be rewritten as Eq. (36).

$$i_c = nFv_c = -nFk_c C_{o,s}^{x,o} exp\left(-\frac{\alpha_c nFE}{RT}\right) \tag{36}$$

In Eq. (35), ka is the anodic rate constant, kc is cathodic rate constant, α_a is the anodic electrochemical transfer coefficient and α_c denotes cathodic electrochemical transfer coefficient. $C_{r,s}$ and $C_{o,s}$, shows the concentrations of the reduced (r) oxidized (o) species formed at interface. While, x,r and x,o are orders of reactions for the reduced and oxidized species respectively.

For an individual redox reaction, the anodic and cathodic electrochemical transfer may be stated as $\alpha_c = 1 - \alpha_a$. Eq. (37) may be used to determine the total current density of a reaction.

$$i = nFk_a C_{r,s}^{x,r} exp\left(\frac{\alpha_a nFE}{RT}\right) - nFk_c C_{o,s}^{x,o} exp\left(-\frac{\alpha_c nFE}{RT}\right) \tag{37}$$

Where, the current density i at equilibrium ($E_{rev.}$) is set equal to zero.

At the surface, the concentrations of chemical species become equal to the respective bulk concentrations (i.e., $C_{r,s} = C_{r,b}$ and $C_{o,s} = C_{o,b}$) in absence of net current. Eq. (38) provides the current density of anodic process, which may also be stated as the exchange current density i_0.

$$i_0 = nFk_a C_{r,s}^{x,r} exp\left(\frac{\alpha_a nFE_{rev}}{RT}\right) - nFk_c C_{o,s}^{x,o} exp\left(-\frac{\alpha_c nFE_{rev}}{RT}\right) \tag{38}$$

Current density can be articulated in terms of the exchange current density and the overvoltage $\eta = E\text{-}E_{rev}$ by combining Eq. (37) and (38) as of Eq. (39)

$$i = i_0\left(\frac{C_{r,s}}{C_{r,b}}\right)^{x,r} e^{\left(\frac{\alpha_a nF(E-E_{rev})}{RT}\right)} - i_0\left(\frac{C_{o,s}}{C_{o,b}}\right)^{x,o} e^{\left(-\frac{\alpha_c nF(E-E_{rev})}{RT}\right)} \tag{39}$$

The ratios $C_{r,s}/C_{r,b}$ and $C_{o,s}/C_{o,b}$ can be obtained through the transport of reactants and products to the metal surface and the colliding interface. There is a variation in surface species concentration from those in the bulk, under the circumstances when mass transport is low as that of charge transfer. Whereas, the low charge transfer rate compared to mass transfer of species, charge control influences the rate of reaction and ratios become equal to unity at the equilibrium potential. In such a situation, Eq. (39) may be reduced to Butler-Volmer Eq. (40).

$$i = i_0 e^{\left(\frac{\alpha_a nF(E-E_{rev})}{RT}\right)} - i_0 e^{\left(-\frac{\alpha_c nF(E-E_{rev})}{RT}\right)} \tag{40}$$

Electrochemical transfer coefficient α is controlled by charge transfer reaction mechanism. Mechanistic considerations may be used to attain their value in different reactions, but this may not be generalized. The slope of plot between potential and logarithm of current density, which is also called empirical Tafel coefficients can be used to determine the transfer coefficient α as shown in Eqs. (41) through (43).

$$\beta_a = \frac{dE}{d\ln i_a};\ \beta_c = \frac{dE}{d\ln i_c} \tag{41}$$

$$\beta_a = \frac{RT}{\alpha_a nF};\ \beta_c = \frac{RT}{\alpha_c nF} \tag{42}$$

Or

$$b_a = \frac{2.303RT}{\alpha_a nF};\ b_c = \frac{2.303RT}{\alpha_c nF} \tag{43}$$

The anodic and cathodic process for a certain redox couple is contained in the above equations. Whereas, only a cathodic or anodic partial current for a given redox process may be enough for corrosion modeling in practice. In some cases, cathodic or anodic partial process may be ignored, like in metal ion reactions, cathodic partial process is ignored because of insignificant accumulation of metal ions in corrosion. Likewise, in case of oxidizing agents, anodic partial process may be ignored for corrosion studies due to focus on reduction process.

5.3.2. Modeling the mass transport

The concentration of reactants and products at the surface and in the bulk or on the interface is controlled by rate of mass transport. Mass transport of species can occur through diffusion, migration, and convection. The significance and dominance of these mechanisms vary with operating conditions and parameters. For instance, migration mechanism may be neglected in case of transport of neutral molecules and charged species. Whereas, in case of an ionic system, migration mechanism becomes significantly important. Nernst diffusion layer may be applied in situations when diffusion mass transfer and convection are dominant. The environment by the corroding surface may be separated into two regions denoted as inner and outer regions. Diffusion mechanism becomes the major controlling mechanism and convection

is negligible in the inner region. Whereas, concentrations of species are uniform and equal to those in the bulk solution in the outer region.

A linear change in concentration of species may be observed from surface to bulk over a certain distance (δ), here δ shows the thickness of diffusion layer. The flux of species i in the locality of a corroding interface can be determined through Fick's law (44)

$$N_i = -D_i\left(\frac{\partial C_i}{\partial z}\right)_{z=0} \tag{44}$$

Where, D_i shows the diffusion coefficient of specie i and z is the direction perpendicular to the surface. By integrating Eq. (44) over the thickness of the diffusion layer gives (45):

$$N_i = -D_i\frac{C_{i,b} - C_{i,s}}{\delta_i} \tag{45}$$

It is worth mentioning that the diffusion layer thickness is not a physical property of the system but is a convenient mathematical construct that helps in distinguishing the dominance of the diffusion and convection. The diffusion layer thickness depends on flow conditions, diffusion coefficient of individual species and properties of the environment and thus has different value for different species. Eq. (45) can be applied to both corrosion products leaving the interface and reactants entering the electrochemical reaction. On combining with Faraday's law, it obtains current density, hence Eq. (45) gives (46).

$$i_c = nFN_O = -nFD_O\frac{C_{O,b} - C_{O,s}}{\delta_O} \tag{46}$$

Current density shows maximum limiting values, as the surface concentration $C_{o,s}$ approaches zero (46). This may be provided as limiting current density (47).

$$i_{c,L} = -\frac{nFD_O C_{O,b}}{\delta_O} \tag{47}$$

An analogous Eq. (48) may be developed for anodic current density for a corrosion product.

$$i_a = nFN_{Me} = -nFD_{Me}\frac{C_{Me,b} - C_{Me,s}}{\delta_{Me}} \tag{48}$$

Due to solubility of corrosion products obtained from Eq. (48) the surface concentration becomes limited. A limiting anodic current density may be attained through Eq. (49), when surface concentration of metal ions corresponds to the metal solubility.

$$i_a = -nFD_{Me}\frac{C_{Me,b} - C_{Me,sat}}{\delta_{Me}} \tag{49}$$

The mixed potential theory or the theory of metal corrosion assists modeling the behavior of the corroding surface. This is sum of all partial anodic currents and is equal to the sum of all partial cathodic currents (Wagner and Traud, 1938). This also assumes that the electrical potential of the metal at both cathodic and anodic sites are equal. This helps in meeting the need of no charge accumulation within the metal. This brings in light that electrons twisted due to oxidation are consumed in reduction process as per Eq. (50).

$$\sum_j A_a i_{a,j} = \sum_j A_c i_{c,j}\,\text{at}\,E = E_{corr} \tag{50}$$

Where, A_a is the area over which anodic reactions take place, A_c indicates area over which cathodic reactions are taking place. Eq. (50) helps in determining the corrosion potential E_{corr}. Using Eq. (51) corrosion rates and the corrosion current density can be calculated with anodic current density from metal dissolution at a given corrosion potential.

$$i_{corr} = i_{a,Me}(E_{corr}) \tag{51}$$

The potential that deviates from the corrosion potential can help in predicting the current. Furthermore, potential relationship versus predicted current may be compared with experimental data obtained for polarization behavior.

Mass transport can also be modelled by using mass transfer coefficients. To calculate the mass transport effect on electrochemical kinetics, it is important to estimate the diffusion layer thickness δ_i or limiting current density. Several empirical relations exist for practical applications of mass transport models. Levich (1962) developed a theoretical solution for rotating disk electrode as shown in Eq. (52) and conformed with experimental results.

$$\delta_i = 1.61 D_i^{1/3}\nu^{1/6}\omega^{-1/2} \tag{52}$$

Where, ω is rotation rate in rad/s, D_i is diffusion coefficient of the reacting species in cm^2/s, and ν is the kinematic viscosity in cm^2/s. The limiting current density may be attained through Eq. (53).

$$i_{c,L} = -0.6205 nFC_{O,b}D_O^{2/3}\nu^{-1/6}\omega^{1/2} \tag{53}$$

Mass transfer coefficients k_m can be obtained by using Eq. (54).

$$k_m = \frac{\text{Reaction rate}}{\text{Concentration driving force}} \tag{54}$$

Eq. (45) for mass-transport and electrochemical reaction rate expressed in current density may be modified in terms of mass transfer coefficient k_m and articulated through Eq. (55).

$$N_i = \frac{i_i}{n_i F} = -D_i\frac{C_{i,b} - C_{i,s}}{\delta_i} = -k_{m,i}\left(C_{i,b} - C_{i,s}\right) \tag{55}$$

Eq. (55) highlights a relationship between diffusion layer thickness (δ_i) and k_m, as shown in equation (56).

$$k_{m,i} = \frac{D_i}{\delta_i} \tag{56}$$

This may also be presented in Sherwood number *Sh*, as per equation (57);

$$Sh = \frac{k_m d}{D} \tag{57}$$

Where, d is a characteristic dimension (e.g., a pipe or rotating disk diameter); Sh; Sherwood number may be associated with Reynolds number (Re) and Schmidt number (Sc), as shown in equations (58) and (59).

$$Re = \frac{Vd}{\nu} \tag{58}$$

$$Sc = \frac{\nu}{D} \tag{59}$$

Where; V shows the linear velocity. The dimensional analysis I indicates that *Sh* is a function of *Re* and *Sc,* which may be expressed as under (60) (Poulson, 1983, 1993):

$$Sh = constant \times Re^x \times Sc^y \tag{60}$$

The theoretical results for a rotating disk may be exhibited as of Eq. (61).

$$Sh = 0.6205 Re^{0.5} Sc^{0.33} \tag{61}$$

Similarly, the correlation of Eisenberg et al. (1954) for a rotating cylindermay be used as of Eq. (62);

$$Sh = 0.0791 Re^{0.7} Sc^{0.356} \tag{62}$$

Berger and Hau (1977) correlation is one of the widely used Eqs. (63) corrosion modeling studies.

$$Sh = 0.0165 Re^{0.86} Sc^{0.33} \tag{63}$$

6. Sample results of corrosion models

Kladkaew et al. (2009) developed an empirical model for estimating

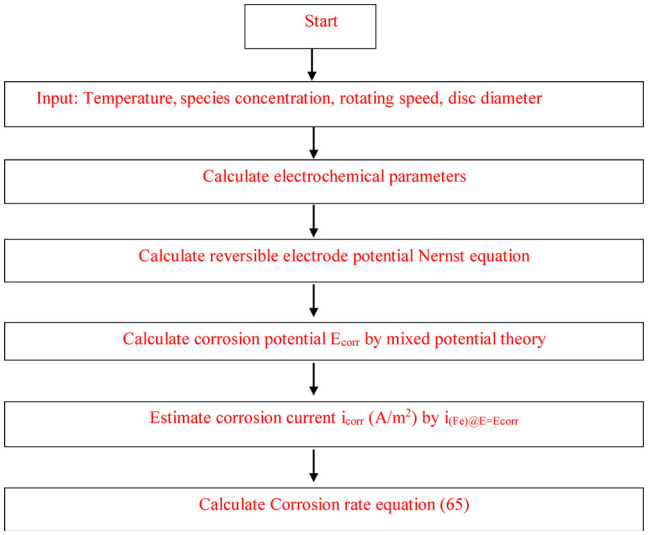

Fig. 2. A simplified flow diagram of steps used by Ghalib et al. (2016) for mechanistic corrosion rate modelling of carbon steel by carbonated MDEA-PZ solutions.

the rate of corrosion for MEA-H_2O-CO_2-O_2-SO_2 system. Model was developed for different concentrations of H_2O, CO_2, O_2 and SO_2 at different temperatures. The empirical model is presented in Eq. (64).

$$CR = 1.77 \times 10^9 \left\{ exp\left[\frac{-5955}{T}\right]\right\} \times \{[SO_2]^{0.0011}[O_2]^{0.0006}[CO_2]^{0.9}[MEA]^{0.0001}\} \quad (64)$$

Where, CR is the rate of corrosion, T is temperature, [MEA], [H_2O], [CO_2], [O_2] and [SO_2] are concentrations of MEA, H_2O, CO_2, O_2 and SO_2 respectively. Model was reported to predict the rate of corrosion of carbon steel with an average absolute deviation percentage (AAD%) of 15.48 %.

Ghalib et al. (2016) previously modelled corrosion behavior of PZ activated MDEA. The model was based on VLE and electrochemical behavior of amine systems. The model predicted speciation of aqueous carbonated MDEA-PZ solutions, their concentrations, activity coefficients, and transport properties. The electrochemical model simulates partial oxidation and reduction processes on the surface of carbon steel. The model predicted the effect of PZ concentration on the carbon steel corrosion rate. A simplified flow diagram of the model development steps is provided in Fig. 2.

$$CR = 1.155 \times i_{corr}(A/m^2) \quad (65)$$

Table 1 presents sample results of rate of corrosion from the model against experimental data for aqueous 1.9 M MDEA + 0.05 M PZ solution.

Veawab and Aroonwilas (2002) proposed a mechanistic model, which can identify oxidizing agents in an aqueous amine CO_2 environment responsible for the rate of corrosion. The concentrations of oxidizing agents were found by incorporating mixed potential theory and electrolyte nonrandom two-liquid (NRTL) equilibrium model. Authors reported that bicarbonate ions and water are major contributing oxidizing agents in corrosion. Fig. 3 shows a comparison of simulated and experimental results of polarization behavior of carbonated aqueous MEA at different temperatures.

Choi et al. (2013) developed a mechanistic corrosion rate model for aqueous CO_2-MDEA system. They used electrochemical reactions and thermodynamic equilibria to develop the predictive model. The results of the model were compared with experimental data. A comparison of experimental results at 50 wt.% MDEA/12 % CO_2 aqueous system at 50 °C to those of modelled are presented in Fig. 4.

Table 1
Comparison of experimental and calculated of carbon steel corrosion data in aqueous 1.9 M MDEA + 0.05 M PZ solution.

T(K)	P_{CO2} (kPa)	Experimental		Model		δ^a	δ^b
		E_{corr} (V)	CR (mmpy)	E_{corr} (V)	CR (mmpy)		
313.15	0.95	−0.84	0.28	−0.82	0.16	2.62	41.49
	9.58	−0.81	0.49	−0.83	0.65	1.28	33.55
	47.55	−0.79	1.44	−0.82	1.26	3.42	12.57
	95.78	−0.79	1.32	−0.80	1.48	1.89	12.75
333.15	0.83	−0.85	0.26	−0.84	0.17	1.98	34.45
	8.29	−0.84	0.63	−0.85	0.74	0.57	18.56
	41.28	−0.81	1.69	−0.84	1.79	4.50	6.18
	83.24	−0.82	1.70	−0.84	2.41	1.94	41.86
353.15	0.55	−0.83	0.18	−0.85	0.14	1.57	23.97
	5.55	−0.83	0.89	−0.86	0.64	3.70	27.78
	27.49	−0.83	1.56	−0.86	1.72	4.37	10.69
	55.64	−0.84	2.02	−0.86	2.57	2.21	27.07

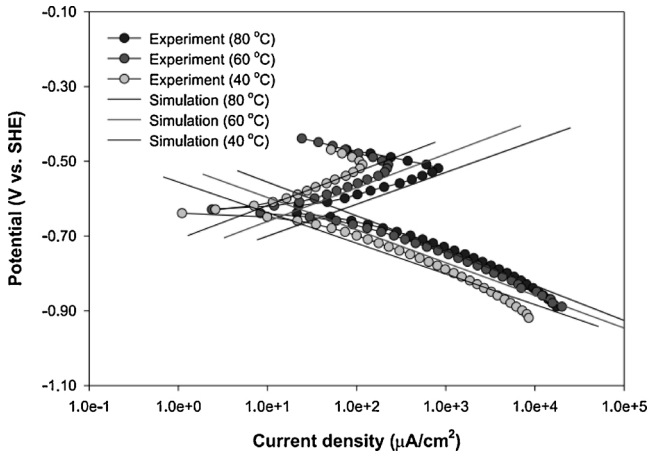

Fig. 3. Polarization behavior of aqueous carbonated MEA at different temperatures (Veawab and Aroonwilas, 2002).

7. Conclusions and outlook

Aqueous CO_2 settings can lead to the occurrence of mesa attack, pitting corrosion, flow-induced corrosion, and uniform corrosion. However, due to complexity of model development for localized corrosion and prevalence of uniform corrosion, most of the corrosion models focus on the uniform corrosion. It is convenient to develop empirical predictive corrosion models. These models are data driven and encompass numerous actual corrosion data through plant operations or laboratory experiments. These models are sometimes linear and other times non-linear mathematical correlations, which include corrosion rate and the operating variables. Due to their simplicity and non-rigorousness these models fall short in extending their application to different systems. This should also be noted that these models require a large set of data for various operating conditions that affect the corrosion rate and their confidence intervals are low, which makes them ineffective for small datapoints. These models extrapolate poorly outside the conditions present in their database, even small variation in data may introduce a large error.

Semi-empirical corrosion rate models are extended versions of empirical models, which include mathematical correlation consisting of an empirical correlation for base corrosion rate and correction factors. The correlations are developed by regressing the corrosion data from plant operations or laboratory experiments. Physical and chemical behavior of corrosion process, for example flow velocity, $FeCO_3$ film formation, pH, and/or the presence of inhibitors is brought in consideration through correction factors. Semi-empirical models use the empirical

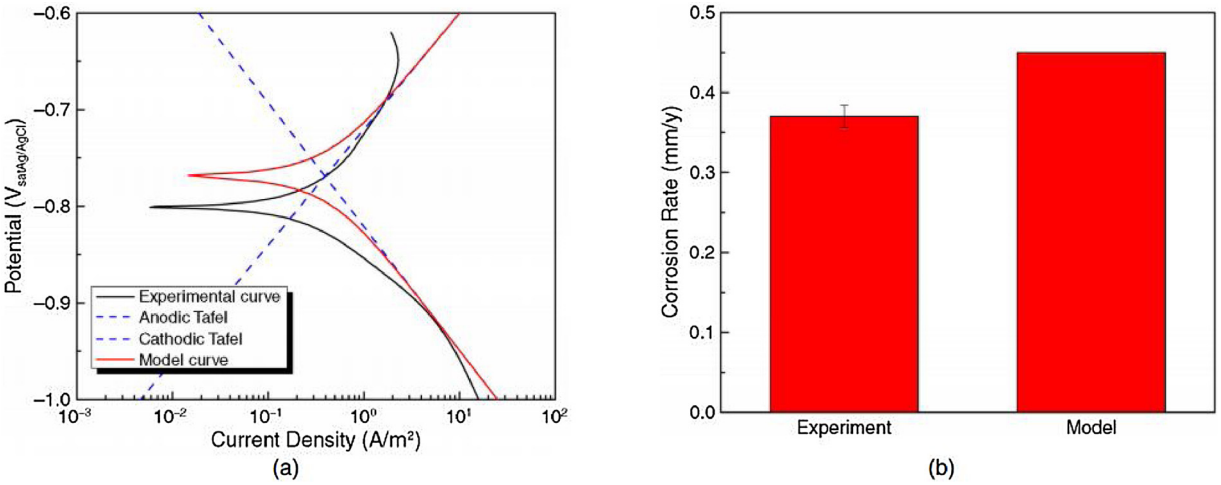

Fig. 4. Comparison of experimental results with modelled (a) polarization curves and (b) corrosion rates by (Choi et al., 2013).

correlations, which require a large set of corrosion data, which is one the drawbacks of such models. However, unlike empirical corrosion rate models, these models are efficient in predicting corrosion rate outside the variable ranges used during model development with higher confidence than the empirical models. These models are preferred by industries as these are less time consuming and simpler to develop than those of rigorous models.

The more rigorous models compared to empirical and semi-empirical are mechanistic corrosion models. These models are developed based on theory of corrosion processes and do not require any corrosion data for the development. These are highly sophisticated models and have very high extrapolation abilities and can be modified for the application of other systems. Such models need an in-depth knowledge of fundamentals of science and engineering related to thermodynamics, reaction kinetics and mass transfer, heat transfer and behavior of degradation products on the rate of corrosion.

Declaration of Competing Interest

The authors declare that they have no known competing financial interests or personal relationships that could have appeared to influence the work reported in this paper.

References

Anderko, A., 2010. Modeling of Aqueous Corrosion, 4 ed. Elsevier, Amsterdam.

Anderko, A., Young, R.D., 1999. Simulation of CO_2/H_2S corrosion using thermodynamic and electrochemical models. Corrosion-National Association of Corrosion Engineers Annual Conference-. NACE.

Aronu, U.E., Hessen, E.T., Haug-Warberg, T., Hoff, K.A., Svendsen, H.F., 2011. Equilibrium absorption of carbon dioxide by amino acid salt and amine amino acid salt solutions. Energy Procedia 4, 109–116.

Austgen Jr., D.M., 1989. A Model of Vapor-liquid Equilibria for Acid Gas-alkanolamine-water Systems. Texas Univ., Austin, TX (USA).

Austgen, D.M., Rochelle, G.T., Peng, X., Chen, C.C., 1989. Model of vapor-liquid equilibria for aqueous acid gas-alkanolamine systems using the electrolyte-NRTL equation. Ind. Eng. Chem. Res. 28, 1060–1073.

Austgen, D.M., Rochelle, G.T., Chen, C.C., 1991. Model of vapor-liquid equilibria for aqueous acid gas-alkanolamine systems. 2. Representation of hydrogen sulfide and carbon dioxide solubility in aqueous MDEA and carbon dioxide solubility in aqueous mixtures of MDEA with MEA or DEA. Ind. Eng. Chem. Res. 30, 543–555.

Bard, A.J., Faulkner, L.R., 1980. Electrochemical Methods: Fundamentals and Applications. Wiley, New York.

Benamor, A., Al-Marri, M.J., 2014. Modeling analysis of corrosion behavior of carbon steel in CO_2 loaded amine solutions. Int. J. Chem. Eng. Appl. 5, 353.

Berger, F., Hau, K.-F.-L., 1977. Mass transfer in turbulent pipe flow measured by the electrochemical method. Int. J. Heat Mass Transf. 20, 1185–1194.

Beutier, D., Renon, H., 1978. Representation of NH_3-H_2S-H_2O, NH3-CO_2-H_2O, and NH_3-SO_2-H_2O vapor-liquid equilibria. Ind. Eng. Chem. Process. Des. Dev. 17, 220–230.

Bockris, J.O.M., Khan, S.U., 2013. Surface Electrochemistry: a Molecular Level Approach. Springer Science & Business Media.

Bockris, J.M., Reddy, A.K., 1970. Modern Electrochemistry: an Introduction to an Interdisciplinary Area Vol. 1 Plenum Press.

Bockris, J.M., Drazic, D., Despic, A., 1961. The electrode kinetics of the deposition and dissolution of iron. Electrochim. Acta 4, 325–361.

Chakma, A., 1997. CO_2 capture processes—opportunities for improved energy efficiencies. Energy Convers. Manage. 38, S51–S56.

Chakma, A., Meisen, A., 1986. Corrosivity of diethanolamine solutions and their degradation products. Ind. Eng. Chem. Prod. Res. Dev. 25, 627–630.

Choi, Y.-S., Nešić, S., Duan, D., Jiang, S., 2012. Mechanistic Modeling of Carbon Steel Corrosion in a MDEA-Based CO_2 Capture Process, CORROSION 2012. NACE International.

Choi, Y.-S., Duan, D., Jiang, S., Nešić, S., 2013. Mechanistic modeling of carbon steel corrosion in a methyldiethanolamine (MDEA)-based carbon dioxide capture process. Corrosion 69, 551–559.

Ciftja, A.F., Hartono, A., da Silva, E.F., Svendsen, H.F., 2011. Study on carbamate stability in the AMP/CO_2/H_2O system from 13C-NMR spectroscopy. Energy Procedia 4, 614–620.

Cross, C., Edwards, D., Santos, J., Steward, E., 1990. Gas treating through the accurate process modeling of speciality amine plants. Laurence Reid Gas Conditioning Conference.

De Waard, C., Lotz, U., 1993. Prediction of CO_2 corrosion of carbon steel. Corrosion-National Association of Corrosion Engineers Annual Conference-. NACE.

De Waard, C., Milliams, D., 1975. Carbonic acid corrosion of steel. Corrosion 31, 177–181.

De Waard, C., Lotz, U., Milliams, D., 1991. Predictive model for CO_2 corrosion engineering in wet natural gas pipelines. Corrosion 47, 976–985.

De Waard, C., Lotz, U., Dugstad, A., 1995. Influence of liquid flow velocity on CO_2 corrosion: a semi-empirical model. Corrosion-National Association of Corrosion Engineers Annual Conference-. NACE.

Deshmukh, R., Mather, A., 1981. A mathematical model for equilibrium solubility of hydrogen sulfide and carbon dioxide in aqueous alkanolamine solutions. Chem. Eng. Sci. 36, 355–362.

Duan, D., Choi, Y.-S., Jiang, S., Nešic, S., 2013. Corrosion Mechanism of Carbon Steel in MDEA-Based CO_2 Capture Plants. CORROSION/2013, Paper.

Dugstad, A., 1998. Mechanism of Protective Film Formation during CO2 Corrosion of Carbon Steel, CORROSION 98. Nace International.

Dugstad, A., Seiersten, M., Nyborg, R., 2003. Flow Assurance of pH Stabilized Wet Gas Pipelines, CORROSION 2003. NACE International.

DuPart, M.S., Bacon, T.R., Edwards, D.J., 1991. Understanding and preventing corrosion in alkanolamine gas treating plants. Proceedings of the 41st Laurance Reid Gas Conditioning Conference 4–6.

DuPart, M., Bacon, T., Edwards, D., 1993. Understanding corrosion in alkanolamine gas treating plants. Hydrocarbon Process. 72, 89–94.

Eisenberg, M., Tobias, C., Wilke, C., 1954. Ionic mass transfer and concentration polarization at rotating electrodes. J. Electrochem. Soc. 101, 306–320.

Evans, S.P., Rosamund, 2019. Mapped: the world's coal power plants. Carbon Brief.

Feng, Z., Jing-Wen, M., Zheng, Z., You-Ting, W., Zhi-Bing, Z., 2012. Study on the absorption of carbon dioxide in high concentrated MDEA and ILs solutions. Chem. Eng. J. 181, 222–228.

Fytianos, G., Ucar, S., Grimstvedt, A., Hyldbakk, A., Svendsen, H.F., Knuutila, H.K., 2016. Corrosion and degradation in MEA based post-combustion CO2 capture. Int. J. Greenh. Gas Control. 46, 48–56.

Gao, J., Wang, S., Sun, C., Zhao, B., Chen, C., 2012. Corrosion behavior of carbon steel at typical positions of an amine-based CO2 capture pilot plant. Ind. Eng. Chem. Res. 51, 6714–6721.

Ghalib, L., Si Ali, B., Mazari, S., Ashri, W.M., Saeed, I.M., 2016. Modeling the effect of piperazine on carbon steel corrosion rate in carbonated activated MDEA solutions. Int. J. Electrochem. Sci. 11, 4560–4585.

Gileadi, E., 1993. Electrode Kinetics for Chemists, Chemical Engineers, and Materials Scientists. Capstone.

Hartley, G., 1935. The application of the Debye-Hückel theory to colloidal electrolytes.

Trans. Faraday Soc. 31, 31–50.
Helle, H., 1995. Corrosion Control in Alkanolamine Gas Treating: Absorber Corrosion. NACE International, Houston, TX (United States).
Kaesche, H., 1985. In: Kaesche, H. (Ed.), Metallic Corrosion, Translated by R. A. Rapp, published 1985 by NACE, 498.
Kahyarian, A., Achour, M., Nesic, S., 2017. Mathematical modeling of uniform CO2 corrosion. Trends in Oil and Gas Corrosion Research and Technologies. Elsevier, pp. 805–849.
Keller, A., Kammiller, R., Veatch, F., Cummings, A., Thompsen, J., Mecum, S., 1992. Heat-stable salt removal from amines by the HSSX process using ion exchange. In: Proceedings of Laurance Reid Gas Conditioning Conference. Norman, OK, USA (2–4 March).
Kent, R., Eisenberg, B., 1976. Paper e, gas conditioning conference, university of oklahoma, 1975. Also. Hydrocarbon Process. 55, 87.
Kittel, J., Idem, R., Gelowitz, D., Tontiwachwuthikul, P., Parrain, G., Bonneau, A., 2009. Corrosion in MEA units for CO 2 capture: pilot plant studies. Energy Procedia 00 (1), 791–797.
Kladkaew, N., Idem, R., Tontiwachwuthikul, P., Saiwan, C., 2009. Corrosion behavior of carbon steel in the monoethanolamine − H_2O − CO_2 − O_2 − SO_2 system: products, reaction pathways, and kinetics. Ind. Eng. Chem. Res. 48, 10169–10179.
Kohl, A.L., Nielsen, R., 1997. Gas Purification. Gulf Professional Publishing.
Kosseim, A., 1984. Corrosion-inhibited amine guard ST process. A. J. Kosseim, et al., (Union Carbide Corp.). Chem. Eng. Prog. 80 (64-71) (1984).
Lee, K.-L., 2004. A Mechanistic Modeling of Carbon Dioxide Corrosion of Mild Steel in the Presence of Hydrogen Sulfide. Doctor of Philosophy College of Engineering and Technology of Ohio University.
Lee, J.I., Otto, F.D., Mather, A.E., 1976. Equilibrium between carbon dioxide and aqueous monoethanolamine solutions. J. Appl. Chem. Biotechnol. 26, 541–549.
Levich, V.G., 1962. Physicochemical Hydrodynamics. Prentice-hall Englewood Cliffs, NJ.
Liang, Z., Fu, K., Idem, R., Tontiwachwuthikul, P., 2016. Review on current advances, future challenges and consideration issues for post-combustion CO_2 capture using amine-based absorbents. Chin. J. Chem. Eng. 24, 278–288.
Liu, X., Zheng, Y., 2008. Effect of hydrophilic group on inhibition behaviour of imidazoline for CO2 corrosion of N80 in 3% NaCl solution. Corros. Eng. Sci. Technol. 43, 87–92.
Luis, P., 2016. Use of monoethanolamine (MEA) for CO_2 capture in a global scenario: consequences and alternatives. Desalination 380, 93–99.
Mac Dowell, N., Samsatli, N., Shah, N., 2013. Dynamic modelling and analysis of an amine-based post-combustion CO_2 capture absorption column. Int. J. Greenh. Gas Control. 12, 247–258.
Mandal, B., Guha, M., Biswas, A., Bandyopadhyay, S., 2001. Removal of carbon dioxide by absorption in mixed amines: modelling of absorption in aqueous MDEA/MEA and AMP/MEA solutions. Chem. Eng. Sci. 56, 6217–6224.
Mazari, S.A., Ali, B.S., Jan, B.M., Saeed, I.M., 2014. Degradation study of piperazine, its blends and structural analogs for CO_2 capture: a review. Int. J. Greenh. Gas Control. 31 (214), 228.
Mazari, S.A., Ali, B.S., Jan, B.M., Saeed, I.M., Nizamuddin, S., 2015. An overview of solvent management and emissions of amine-based CO_2 capture technology. Int. J. Greenh. Gas Control. 34, 129–140.
Milton, R.M., 1963. Sweetening and drying of natural gas. Google Patents.
Mishra, B., Al-Hassan, S., Olson, D., Salama, M., 1997. Development of a predictive model for activation-controlled corrosion of steel in solutions containing carbon dioxide. Corrosion 53, 852–859.
Mock, B., Evans, L., Chen, C.C., 1986. Thermodynamic representation of phase equilibria of mixed-solvent electrolyte systems. AIChE J. 32, 1655–1664.
Murata, R., Benaquisto, J., Storey, C., 2015. A methodology for identifying and addressing dead-legs and corrosion issues in a process Hazard Analysis (PHA). J. Loss Prev. Process Ind. 35, 387–392.
Najumudeen, A., 2012. Development of a Mechanistic Corrosion Model for Carbon Steel in MEA-based CO2 Absorption Process. Faculty of Graduate Studies and Research, University of Regina.
Nešić, S., 2007. Key issues related to modelling of internal corrosion of oil and gas pipelines–a review. Corros. Sci. 49, 4308–4338.
Nešic, S., Lee, K.-L., 2003. A mechanistic model for carbon dioxide corrosion of mild steel in the presence of protective iron carbonate films—part 3: film growth model. Corrosion 59, 616–628.
Nesic, S., Nordsveen, M., Maxwell, N., Vrhovac, M., 2001a. Probabilistic modelling of CO_2 corrosion laboratory data using neural networks. Corros. Sci. 43, 1373–1392.
Nesic, S., Nyborg, R., Stangeland, A., Nordsveen, M., 2001b. Mechanistic Modeling for CO_2 Corrosion with Protective Iron carbonate Films, CORROSION 2001. NACE International.
Nešić, S., Lee, J., Ruzic, V., 2002. A Mechanistic Model of Iron Carbonate Film Growth and the Effect on CO_2 Corrosion of Mild Steel. Corrosion/02, Paper.
Nešić, S., Li, H., Huang, J., Sormaz, D., 2009. An open source mechanistic model for CO_2/H_2S corrosion of carbon steel. Corrosion 2009.
Nielsen, R., Lewis, K., McCullough, J.G., Hansen, D., 1995. Controlling corrosion in amine treating plants. In: Proceedings of the Laurance Reid Gas Conditioning Conference. Norman, Oklahoma.
Nouri, M., Mesbah, J., Shaibani, S.B., 2008. A Verified Computer Model for Corrosion Rate Prediction in a Di-ethanol Amine System Using Field Data, CORROSION 2008. NACE International.
Nyborg, R., 2002. Overview of CO_2 Corrosion Models for Wells and Pipelines, CORROSION 2002. NACE International.
Observatory, M.L., 2019. Trends in Atmospheric Carbon Dioxide. https://www.esrl.noaa.gov/gmd/ccgg/trends/.
Oko, E., Wang, M., Joel, A.S., 2017. Current status and future development of solvent-based carbon capture. Int. J. Coal Sci. Technol. 4, 5–14.
Pots, B.F., Kapusta, S.D., John, R.C., Thomas, M., Rippon, I.J., Whitham, T., Girgis, M., 2002. Improvements on De Waard-Milliams Corrosion Prediction and Applications to Corrosion Management, CORROSION 2002. Nace International.
Poulson, B., 1983. Electrochemical measurements in flowing solutions. Corros. Sci. 23, 391–430.
Poulson, B., 1993. Advances in understanding hydrodynamic effects on corrosion. Corros. Sci. 35, 655–665.
Riesenfeld, F., Blohm, C., 1950. Corrosion problems in gas purification units employing MEA solutions. Petroleum Refiner 20, 141–150.
Rochelle, G.T., 2009. Amine scrubbing for CO_2 capture. Science 325, 1652–1654.
Roger, B.R., 1930. Process for separating acidic gases. Google Patents.
Roger, B.R., 1931. Process for separating acidic gases. Google Patents.
Saeed, I.M., Alaba, P., Mazari, S.A., Basirun, W.J., Lee, V.S., Sabzoi, N., 2018. Opportunities and challenges in the development of monoethanolamine and its blends for post-combustion CO_2 capture. Int. J. Greenh. Gas Control. 79, 212–233.
Soosaiprakasam, I., 2007. Corrosion Inhibition Performance of Copper Carbonate in Carbon Dioxide Absorption Process Using Aqueous Solution of Monoethanolamine. Regina.
Soosaiprakasam, I.R., Veawab, A., 2008. Corrosion and polarization behavior of carbon steel in MEA-based CO2 capture process. Int. J. Greenh. Gas Control. 2, 553–562.
Tanthapanichakoon, W., Veawab, A., 2003. Heat stable salts and corrosivity in amine treating units. Greenhouse Gas Control Technologies-6th International Conference. Pergamon, Oxford, pp. 1591–1594.
Tanthapanichakoon, W., Veawab, A., McGarvey, B., 2006. Electrochemical investigation on the effect of heat-stable salts on corrosion in CO2 capture plants using aqueous solution of MEA. Ind. Eng. Chem. Res. 45, 2586–2593.
Veawab, A., Aroonwilas, A., 2002. Identification of oxidizing agents in aqueous amine–CO2 systems using a mechanistic corrosion model. Corros. Sci. 44, 967–987.
Veawab, A., Tontiwachwuthikul, P., Chakma, A., 1999. Corrosion behavior of carbon steel in the CO2 absorption process using aqueous amine solutions. Ind. Eng. Chem. Res. 38, 3917–3924.
Vetter, K.J., 2013. Electrochemical Kinetics: Theoretical Aspects. Elsevier.
Videm, K., Dugstad, A., 1989. Corrosion of carbon steel in an aqueous carbon dioxide environment. I: solution effects. Mater. Perform. 28, 63–67.
Wagner, C., Traud, W., 1938. Z. Elektrochem. Angew. Physik. Chem 44, 391.
Wattanaphan, P., Sema, T., Idem, R., Liang, Z., Tontiwachwuthikul, P., 2013. Effects of flue gas composition on carbon steel (1020) corrosion in MEA-based CO_2 capture process. Int. J. Greenh. Gas Control. 19, 340–349.
Yang, L., 2008. Techniques for Corrosion Monitoring. Elsevier.
Zheng, L., Matin, N.S., Landon, J., Thomas, G.A., Liu, K., 2016a. CO_2 loading-dependent corrosion of carbon steel and formation of corrosion products in anoxic 30 wt.% monoethanolamine-based solutions. Corros. Sci. 102, 44–54.
Zheng, L., Matin, N.S., Thompson, J., Landon, J., Holubowitch, N.E., Liu, K., 2016b. Understanding the corrosion of CO_2-loaded 2-amino-2-methyl-1-propanol solutions assisted by thermodynamic modeling. Int. J. Greenh. Gas Control. 54, 211–218.